

Age, Association and Provenance of the “Neoproterozoic” Fengshuigouhe Group in the Northwestern Lesser Xing’an Range, NE China: Constraints from Zircon U-Pb Geochronology

Meijun Xu (徐美君), Wenliang Xu* (许文良), Feng Wang (王枫), Fuhong Gao (高福红)

College of Earth Sciences, Jilin University, Changchun 130061, China

ABSTRACT: The formation time of the Fengshuigouhe (风水沟河) Group in the northwestern Lesser Xing’an Range (小兴安岭), NE China, remains controversial owing to the lack of precise dating data. This article reports zircon U-Pb ages for the leptynite and gneissic granitoids from the Fengshuigouhe Group in the northwestern Lesser Xing’an Range. The aim is to constrain the formation time and provenance of Fengshuigouhe Group. Field observation indicates that the Fengshuigouhe Group consists of a suite of metamorphic rocks (leptynite) and gneissic granitoids intruding the leptynite, and that both of them are cut by late granitic pegmatite. Zircons from two leptynites are euhedral-subhedral in shape and display oscillatory zoning in CL (cathodoluminescence) images. These detrital zircons give weighted mean ages of 255, 291, 321, 361, 469, and 520 Ma. The youngest age of them is interpreted to maximum depositional age of the protoliths of these leptynites. Zircons from gneissic granites are euhedral and subhedral in shape and exhibit typical oscillatory zoning in CL images. The dating results indicate that the gneissic granites were formed in the Early Jurassic (185±2 Ma). Zircons from the late granitic pegmatite are subhedral in shape and exhibit two types in CL images: structureless and oscillatory zoning. The former gives a weighted mean age of 143±1 Ma, considered to represent the timing of crystallization of the pegmatite, the latter yield several groups of ages: 178, 273, 319, 482, 611, and 788 Ma, representing the crystallization age of inherited or captured zircons entrained by the pegmatite. Taken together, we conclude that the Fengshuigouhe Group in the northwestern Lesser Xing’an Range formed between Late Paleozoic (255 Ma) to Early Mesozoic (185 Ma), rather than Neoproterozoic as previously believed, and that the sediments in the Fengshuigouhe Group were sourced directly from geological bodies in the study area and adjacent regions.

KEY WORDS: the Lesser Xing’an Range, Fengshuigouhe Group, formation time, leptynite, zircon U-Pb geochronology.

This study was financially supported by the National Natural Science Foundation of China (No. 41072038), China Geological Survey (No. 1212010070301), and the Opening Foundation of the State Key Laboratory of Geological Processes and Mineral Resources, China University of Geosciences, Wuhan.

*Corresponding author: xuwl@jlu.edu.cn

© China University of Geosciences and Springer-Verlag Berlin Heidelberg 2012

Manuscript received March 21, 2012.

Manuscript accepted September 8, 2012.

INTRODUCTION

Northeast China is located in the eastern segment of the Central Asian orogenic belt (CAOB). The Pa-

leozoic tectonic evolution of NE China was characterized by the amalgamation of microcontinental massifs and the closing of Paleo-Asiatic Ocean in this region (Xu et al., 2009; Wu et al., 2007a, 2002; Li, 2006; Li et al., 1999). It remains controversial whether the Precambrian metamorphic crystalline basements exist within the several microcontinental massifs. Traditionally, the Precambrian metamorphic basements exist in each microcontinental massif, such as the Xinghuadukou Group in the Erguna massif, the Mashan Group in the Jiamusi massif, the Zhangguangcailing Group in the Songnen-Zhangguangcai Range massif (HBGMR, 1993), the Zhalantun Group and the Xilin Gol complex in Xing'an massif (IMBGMR, 1991). However, recent zircon U-Pb dating results indicate that these so-called Precambrian strata actually formed in Paleozoic and Early Mesozoic. For example, the Mashan Group in the Jiamusi massif actually formed in Early Paleozoic (Wu et al., 2007a; Wilde et al., 2003, 2000), the previously thought Paleoproterozoic Xilin Gol complex in Central Inner Mongolia formed in the Palaeozoic (Chen et al., 2009; Shi et al., 2004), the Xinkailing-Keluo complex in the Xing'an massif and the Xinghuadulou Group in the Erguna massif also formed in the Palaeozoic (Miao et al., 2007, 2003), the Zhangguangcailing Group in the Songnen-Zhangguangcai Range massif is a tectonic mélange that formed in Early Paleozoic to Early Mesozoic (Wang et al., 2012, 2011), and the previously believed Paleoproterozoic Heilongjiang complex is also a tectonic mélange emplaced during Early–Middle Jurassic (Zhou et al., 2009; Wu et al., 2007a). Then, when did the Fengshuigouhe Group, occurred in the northwestern Lesser Xing'an Range and one of the Precambrian strata in NE China, form? Previously believed Neoproterozoic, Paleozoic, or Mesozoic? As a result, this article reports the zircon U-Pb dating results from the Neoproterozoic Fengshuigouhe Group in the Xing'an massif. These data provide important constraints on both the formation timing of the Fengshuigouhe Group and tectonic evolution of the Xing'an massif.

GEOLOGICAL BACKGROUND AND SAMPLE DESCRIPTIONS

The study area is located within the Xing'an mas-

sif and is adjacent to the Hegenshan-Heihe suture zone between the Xing'an and Songnen-Zhangguangcai Range massifs (Fig. 1a). The outcropping strata in the study area include the Neoproterozoic Fengshuigouhe Group which consists of leptynite, gneiss and schist (HBGMR, 1993), the Preordovician Beishihe Formation, the Carboniferous Heibeizi, Kunaerhe, Hetaoshan formations, the Permian Wudaoling Formation, the Jurassic Tamulan'gou, Shangkuli formations, and the Cretaceous Jiufengshan, Ganhe, Xigangzi, Nenjiang, Yuliangzi formations. In addition, voluminous Paleozoic–Mesozoic and minor Proterozoic granitoids occur in this area (HBGMR, 1991, 1978).

The Fengshuigouhe Group is composed mainly of schist, gneiss, leptynite, and felsic hornfels as well as marble interbed (HBGMR, 1991, 1978).

Samples HSW6 are collected near the highway from Sunwu County to Xigangzi Town ($49^{\circ}43'07.0''N$, $127^{\circ}20'22.6''E$) (Fig. 1b), whereas sample 11HSW4-2 is collected from the standard section in the northeastern of Maihai Town ($49^{\circ}18'05.9''N$, $126^{\circ}35'18.4''E$) (HBGMR, 1993) (Fig. 1c). In the location of samples HSW6, field observation indicates that the Fengshuigouhe Group consists of leptynite with layer structure, gneissic granite intruding the leptynite, and pegmatite intruding the previous both (Fig. 2). All selected samples are described below.

Samples HSW6-1 and 11HSW4-2, biotite leptynites (Fig. 3a), are dark grey in color, and display a lepido-granoblastic texture and weak schistose structure, and are composed mainly of plagioclase (~40%), quartz (~48%) and minor amounts of biotite (~10%). Accessory minerals include zircon, magnetite, and apatite.

Samples HSW6-4 and HSW6-12, gneissic biotite syenogranites (Fig. 3b), are pale red in color, display a fine-medium grained granitic texture and weak gneissic structure, and consist of orthoclase (~50%), quartz (~28%), plagioclase (~15%), and biotite (~5%), as well as minor amounts of accessory minerals such as zircon, magnetite and apatite.

Sample HSW6-9, a granitic pegmatite, is pale red in color, and displays pegmatitic texture and massive structure, and consists of quartz and alkali feldspar.

ANALYTICAL METHODS

Zircons were separated from samples using the

conventional heavy liquid and magnetic techniques and purified by handpicking under a binocular microscope at the Langfang Regional Geophysical Survey, Hebei Province, China. The handpicked zircons were examined under transmitted and reflected light with an optical microscope. Transmitted light, reflected light, and cathodoluminescence (CL) images were collected on a microscope and a JEOL scanning electron microscope, respectively, at the State Key Laboratory of Continental Dynamics, Northwestern University, Xi'an, China. The LA-ICP-MS zircon U-Pb analyses were conducted on an Agilent 7500a ICP-MS equipped with a 193 nm laser, housed at the State Key Laboratory of Geological Processes and Mineral Resources, China University of

Geosciences, Wuhan. Zircon 91500 was used as external standard for age calibration and the NIST SRM 610 silicate glass was applied for the instrument optimization. The crater diameter was 32 μm during the analyses. The instrument parameter and detail procedures were described by Liu et al. (2010a, b, 2008). The ICPMSDataCal (Ver. 6.7, Liu et al., 2010a, 2008) and Isoplot (Ver. 3.0, Ludwig, 2003) programs were used for data reduction. Correction for common Pb was made following Anderson (2002). Errors on individual analyses by LA-ICP-MS are quoted at the 1σ level. LA-ICP-MS U-Pb analytical results of zircons in this article are listed in Table 1.

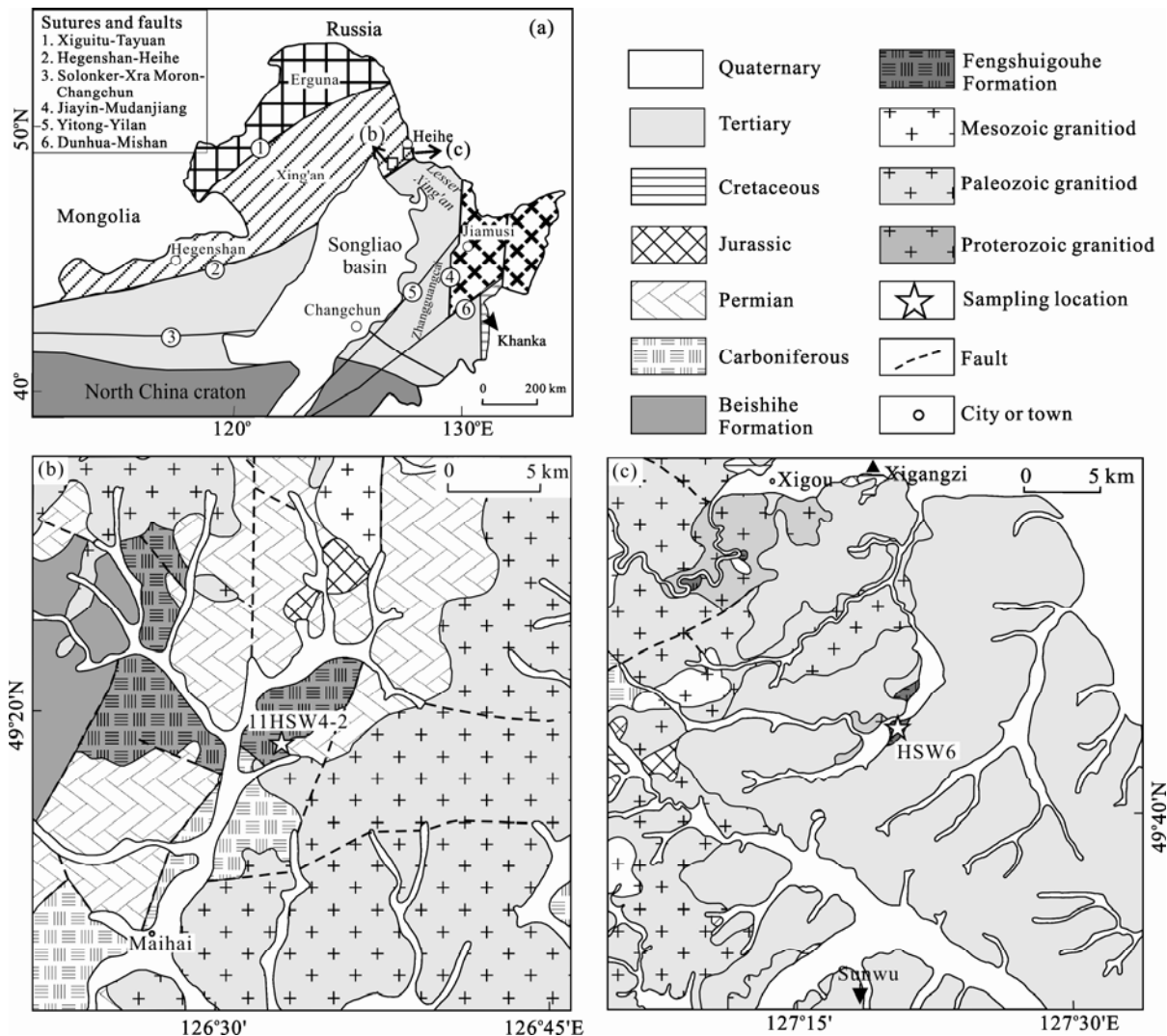


Figure 1. (a) Tectonic sketch map of NE China (modified after Wu et al., 2007b); **(b)** geological map of the Maihai Town in Heihe City; **(c)** geological map of the Xigangzi Town in Heihe City.

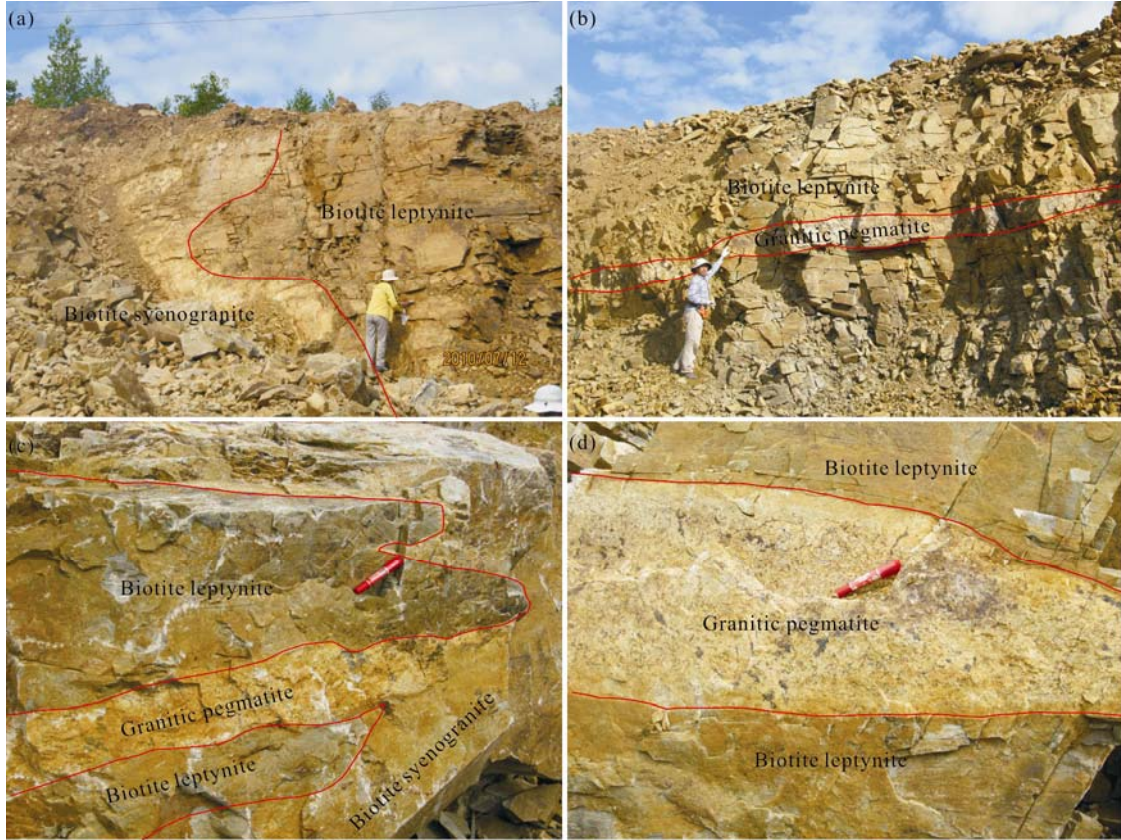


Figure 2. Photographs showing field relationship of the leptynite, granite and pegmatite from the Fengshuigouhe Group. (a) Biotite syenogranite intrudes into biotite leptynite; (b) biotite leptynite is cut by late granitic pegmatite dyke; (c) biotite leptynite and biotite syenogranite are cut by late granitic pegmatite; (d) biotite leptynite is cut by late granitic pegmatite.

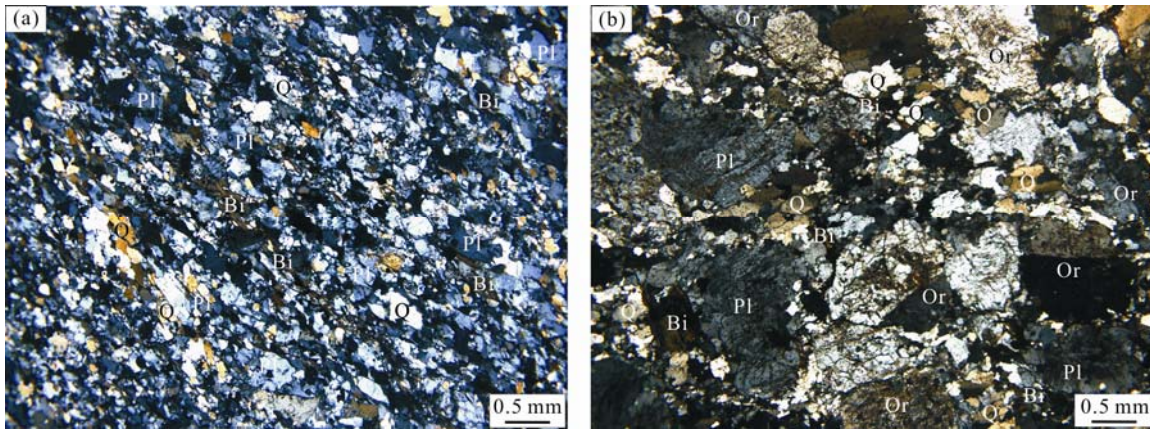


Figure 3. Photomicrographs showing petrography of selected samples from the Fengshuigouhe Group. (a) Biotite leptynite; (b) gneissic biotite syenogranite. Bi. biotite; Or. orthoclase; Pl. plagiocalse; Q. quartz.

RESULTS OF U-PB DATING

Biotite Leptynite

Zircons from leptynites (HSW6-1 and 11HSW4-2) are mostly euhedral-subhedral in shape and display oscillatory zoning in CL images, implying their magmatic origin (Figs. 4a and 4b). The dating

results indicate that the $^{206}\text{Pb}/^{238}\text{U}$ ages of zircons from the sample HSW6-1 range from 249 to 325 Ma, yielding three groups of concordia ages: 255 ± 5 ($n=7$, 1σ), 291 ± 2 ($n=20$, 1σ), and 320 ± 4 Ma ($n=6$, 1σ) (Fig. 5a, Table 1), whereas those zircons from the sample 11HSW4-2 vary from 251 to 554 Ma, yielding

Table 1 LA-ICP-MS zircon U-Pb dating from the Fengshiguouhe Group

Spot	232Th (ppm)	238U (ppm)	Th/U	Isotopic ratios						207Pb/235U	207Pb/206Pb	207Pb/206Pb	206Pb/238U				
				207Pb/206Pb		207Pb/235U		206Pb/238U									
				Ratio	1 σ	Ratio	1 σ	Ratio	1 σ								
HSW6-1-01	92	249	0.37	0.05451	0.0033	0.34561	0.02045	0.04599	0.0006	392	140	301	15	290	4		
HSW6-1-02	137	120	1.14	0.04750	0.0051	0.29718	0.0313	0.04537	0.0008	75	225	264	25	286	5		
HSW6-1-03	155	189	0.82	0.05402	0.0034	0.34546	0.0223	0.04622	0.0006	372	122	301	17	291	4		
HSW6-1-04	717	504	1.42	0.05770	0.0023	0.37147	0.0148	0.04624	0.0005	518	68	321	11	291	3		
HSW6-1-05	106	195	0.54	0.04994	0.0063	0.31791	0.0396	0.04617	0.0010	192	269	280	31	291	6		
HSW6-1-06	118	283	0.42	0.04865	0.0062	0.26498	0.0336	0.03950	0.0007	131	263	239	27	250	4		
HSW6-1-07	72	92	0.78	0.05229	0.0077	0.33532	0.0485	0.04651	0.0010	298	313	294	37	293	6		
HSW6-1-08	350	1194	0.29	0.05300	0.0020	0.30359	0.0113	0.04154	0.0004	329	89	269	9	262	3		
HSW6-1-09	210	391	0.54	0.05566	0.0021	0.39023	0.0161	0.05084	0.0008	439	64	335	12	320	5		
HSW6-1-10	296	279	1.06	0.05466	0.0028	0.34585	0.0185	0.04604	0.0007	398	94	302	14	290	4		
HSW6-1-11	78	145	0.54	0.05354	0.0055	0.33471	0.0322	0.04612	0.0010	352	177	293	24	291	6		
HSW6-1-12	378	396	0.96	0.05233	0.0020	0.36697	0.0145	0.05080	0.0006	300	67	317	11	319	4		
HSW6-1-13	301	215	1.40	0.06364	0.0043	0.39998	0.0250	0.04621	0.0007	730	109	342	18	291	4		
HSW6-1-14	249	517	0.48	0.06254	0.0028	0.34719	0.0171	0.04015	0.0009	693	68	303	13	254	5		
HSW6-1-15	154	461	0.33	0.06754	0.0030	0.42870	0.0178	0.04612	0.0005	855	68	362	13	291	3		
HSW6-1-16	184	395	0.47	0.04605	0.0037	0.25566	0.0196	0.04027	0.0009	175	231	16	254	6			
HSW6-1-17	215	208	1.04	0.06040	0.0060	0.38404	0.0375	0.04612	0.0009	618	223	330	28	291	5		
HSW6-1-18	109	104	1.05	0.05852	0.0044	0.36833	0.0270	0.04618	0.0010	549	123	318	20	291	6		
HSW6-1-19	218	248	0.88	0.08283	0.0052	0.51820	0.0299	0.04599	0.0008	1265	84	424	20	290	5		
HSW6-1-20	160	166	0.96	0.05316	0.0037	0.33517	0.0219	0.04598	0.0007	336	120	294	17	290	5		
HSW6-1-21	197	255	0.77	0.07115	0.0056	0.44804	0.0377	0.04642	0.0014	962	122	376	26	293	9		
HSW6-1-22	254	569	0.45	0.05351	0.0029	0.34459	0.0189	0.04628	0.0008	350	94	301	14	292	5		
HSW6-1-23	68	211	0.32	0.04725	0.0052	0.25848	0.0275	0.03967	0.0010	62	230	233	22	251	6		
HSW6-1-24	247	263	0.94	0.05441	0.0033	0.37924	0.0218	0.05040	0.0009	388	97	326	16	317	6		
HSW6-1-25	101	186	0.54	0.05055	0.0058	0.27432	0.0311	0.03936	0.0008	221	259	246	25	249	5		
HSW6-1-26	751	492	1.53	0.05092	0.0023	0.32456	0.0149	0.04625	0.0007	237	80	285	11	291	4		

Continued

Spot	^{232}Th (ppm)	^{238}U (ppm)	Th/U	Isotopic ratios								$^{207}\text{Pb}/^{206}\text{Pb}$	$^{207}\text{Pb}/^{235}\text{U}$	$^{206}\text{Pb}/^{238}\text{U}$	$^{207}\text{Pb}/^{206}\text{Pb}$	$^{207}\text{Pb}/^{235}\text{U}$	$^{206}\text{Pb}/^{238}\text{U}$				
				$^{207}\text{Pb}/^{206}\text{Pb}$				$^{207}\text{Pb}/^{235}\text{U}$													
				Ratio	1σ	Ratio	1σ	Ratio	1σ	Age (Ma)	1σ										
HSW6-1-27	601	417	1.44	0.046 89	0.004 1	0.299 11	0.025 5	0.046 26	0.000 7	44	191	266	20	292	4						
HSW6-1-28	241	411	0.59	0.052 01	0.003 5	0.330 54	0.021 9	0.046 10	0.000 6	286	156	290	17	291	4						
HSW6-1-29	77	96	0.81	0.048 39	0.004 8	0.339 77	0.032 8	0.050 92	0.000 9	119	219	297	25	320	5						
HSW6-1-30	125	280	0.45	0.061 93	0.004 4	0.441 24	0.033 4	0.050 53	0.001 1	672	125	371	24	318	7						
HSW6-1-31	302	475	0.63	0.052 80	0.003 0	0.337 42	0.018 8	0.046 18	0.000 7	320	100	295	14	291	4						
HSW6-1-32	143	220	0.65	0.069 11	0.010 6	0.492 54	0.075 1	0.051 69	0.001 1	902	340	407	51	325	7						
HSW6-1-33	1 272	833	1.53	0.054 85	0.002 3	0.304 92	0.013 0	0.040 14	0.000 7	406	65	270	10	254	4						
HSW6-4-01	204	220	0.93	0.065 38	0.005 6	0.416 54	0.037 2	0.046 05	0.000 9	787	158	354	27	290	5						
HSW6-4-02	94	284	0.33	0.051 77	0.003 4	0.205 81	0.013 8	0.028 83	0.000 8	275	105	190	12	183	5						
HSW6-4-03	38	180	0.21	0.054 92	0.006 1	0.268 27	0.029 1	0.035 43	0.000 8	409	253	241	23	224	5						
HSW6-4-04	46	61	0.75	0.074 27	0.012 1	0.262 28	0.036 0	0.029 03	0.001 0	1 049	227	237	29	184	6						
HSW6-4-05	206	433	0.48	0.050 85	0.003 5	0.199 96	0.013 2	0.028 99	0.000 5	234	121	185	11	184	3						
HSW6-4-06	970	622	1.56	0.055 72	0.002 2	0.354 60	0.012 9	0.046 16	0.000 5	441	63	308	10	291	3						
HSW6-4-07	429	1 210	0.35	0.055 52	0.001 7	0.277 27	0.008 1	0.036 21	0.000 4	433	44	248	6	229	3						
HSW6-4-08	186	140	1.33	0.056 13	0.004 8	0.391 34	0.031 9	0.050 97	0.001 1	457	144	335	23	321	7						
HSW6-4-09	283	716	0.39	0.052 40	0.002 6	0.333 08	0.016 1	0.046 10	0.000 5	303	116	292	12	291	3						
HSW6-4-10	106	305	0.35	0.058 12	0.004 9	0.233 30	0.019 0	0.029 11	0.000 6	534	191	213	16	185	4						
HSW6-4-11	113	199	0.57	0.056 98	0.006 4	0.220 88	0.026 9	0.029 05	0.001 3	491	192	203	22	185	8						
HSW6-4-12	77	308	0.25	0.052 36	0.002 9	0.276 09	0.016 5	0.038 45	0.000 9	301	93	248	13	243	6						
HSW6-4-13	133	85	1.57	0.078 44	0.008 1	0.313 75	0.032 9	0.027 81	0.000 7	1 158	167	277	25	177	5						
HSW6-4-14	187	529	0.35	0.054 15	0.002 0	0.402 61	0.016 5	0.053 49	0.001 1	377	56	344	12	336	7						
HSW6-4-15	35	137	0.25	0.056 72	0.005 1	0.300 16	0.021 8	0.039 93	0.000 9	481	119	267	17	252	6						
HSW6-4-16	590	1 365	0.43	0.051 84	0.001 5	0.254 15	0.007 0	0.035 33	0.000 4	278	45	230	6	224	2						
HSW6-4-17	199	371	0.54	0.070 51	0.008 7	0.282 66	0.034 0	0.029 07	0.000 8	943	265	253	27	185	5						
HSW6-4-18	60	551	0.11	0.053 27	0.002 3	0.242 26	0.010 3	0.032 91	0.000 4	340	76	220	8	209	2						
HSW6-4-19	492	1 264	0.39	0.051 46	0.001 9	0.207 50	0.008 0	0.029 15	0.000 5	261	59	191	7	185	3						

Continued

Spot	(ppm)	^{238}U (ppm)	Th/U	Isotopic ratios						$^{206}\text{Pb}/^{238}\text{U}$					
				$^{207}\text{Pb}/^{206}\text{Pb}$		$^{207}\text{Pb}/^{235}\text{U}$		$^{206}\text{Pb}/^{238}\text{U}$		$^{207}\text{Pb}/^{206}\text{Pb}$		$^{207}\text{Pb}/^{235}\text{U}$		$^{206}\text{Pb}/^{238}\text{U}$	
				Ratio	1σ	Ratio	1σ	Ratio	1σ	Age (Ma)	1σ	Age (Ma)	1σ	Age (Ma)	
HSW6-4-20	362	571	0.63	0.051 05	0.002 1	0.324 29	0.013 3	0.046 02	0.000 7	243	66	285	10	290	4
HSW6-4-21	92	558	0.17	0.055 11	0.002 9	0.223 16	0.012 2	0.029 28	0.000 5	417	92	205	10	186	3
HSW6-4-22	175	129	1.35	0.071 44	0.008 0	0.260 66	0.025 0	0.028 97	0.001 0	970	142	235	20	184	6
HSW6-4-23	60	249	0.24	0.051 00	0.003 6	0.277 99	0.019 4	0.039 54	0.000 6	241	164	249	15	250	4
HSW6-4-24	119	1 290	0.09	0.051 72	0.002 3	0.201 94	0.008 6	0.028 32	0.000 3	273	103	187	7	180	2
HSW6-4-25	662	561	1.18	0.050 18	0.003 2	0.199 23	0.012 5	0.029 07	0.000 5	203	110	184	11	185	3
HSW6-9-01	111	288	0.39	0.052 53	0.003 0	0.367 03	0.020 4	0.050 67	0.000 7	309	133	317	15	319	4
HSW6-9-02	229	641	0.36	0.048 53	0.002 1	0.291 04	0.013 5	0.043 08	0.000 7	125	77	259	11	272	4
HSW6-9-03	345	3 174	0.11	0.055 98	0.002 5	0.173 72	0.007 6	0.022 51	0.000 2	451	103	163	7	143	1
HSW6-9-04	474	3 861	0.12	0.056 19	0.002 0	0.176 17	0.005 8	0.022 60	0.000 3	460	47	165	5	144	2
HSW6-9-05	95	293	0.32	0.062 68	0.004 2	0.370 31	0.023 4	0.043 20	0.000 9	697	101	320	17	273	5
HSW6-9-06	3 260	5 238	0.62	0.079 58	0.002 9	0.245 70	0.006 9	0.022 61	0.000 4	1 187	31	223	6	144	2
HSW6-9-07	16 346	10 529	1.55	0.051 91	0.002 1	0.169 76	0.009 5	0.023 47	0.000 9	281	63	159	8	150	6
HSW6-9-08	377	435	0.87	0.065 92	0.002 1	0.907 88	0.027 9	0.099 43	0.001 1	804	46	656	15	611	6
HSW6-9-09	221	738	0.30	0.057 48	0.001 5	0.616 90	0.016 1	0.077 61	0.001 0	510	36	488	10	482	6
HSW6-9-10	3 567	13 359	0.27	0.054 91	0.002 3	0.168 67	0.006 8	0.022 28	0.000 3	408	97	158	6	142	2
HSW6-9-11	18 627	18 659	1.00	0.058 53	0.001 5	0.225 77	0.005 6	0.027 98	0.000 3	755	544	231	54	183	7
HSW6-9-12	218 314	82 502	2.65	0.051 06	0.001 1	0.160 41	0.005 0	0.022 67	0.000 6	243	33	151	4	144	4
HSW6-9-13	4 667	12 229	0.38	0.050 60	0.001 3	0.157 97	0.006 0	0.022 41	0.000 6	223	44	149	5	143	4
HSW6-9-14	215	254	0.85	0.069 13	0.002 2	1.241 50	0.037 7	0.130 10	0.001 3	903	46	820	17	788	8
HSW6-9-15	5 022	4 988	1.01	0.068 82	0.003 1	0.215 52	0.009 0	0.022 57	0.000 5	893	52	198	7	144	3
HSW6-9-16	785	4 621	0.17	0.171 26	0.004 4	0.659 75	0.015 4	0.027 97	0.000 4	550	59	207	5	178	2
HSW6-9-17	930	7 004	0.13	0.056 19	0.002 1	0.178 11	0.006 2	0.022 81	0.000 3	460	51	166	5	145	2
HSW6-9-18	1 083	2 601	0.42	0.051 79	0.001 4	0.312 34	0.008 7	0.043 31	0.000 5	276	42	276	7	273	3
HSW6-9-19	23 442	78 719	0.30	0.050 49	0.001 0	0.155 37	0.003 1	0.022 12	0.000 3	218	23	147	3	141	2
HSW6-9-20	807	2 054	0.39	0.069 70	0.006 0	0.221 36	0.018 1	0.023 03	0.000 6	920	184	203	15	147	4

Continued

Spot	^{232}Th		^{238}U		Th/U		$^{207}\text{Pb}/^{206}\text{Pb}$		$^{207}\text{Pb}/^{235}\text{U}$		$^{206}\text{Pb}/^{238}\text{U}$		$^{207}\text{Pb}/^{206}\text{Pb}$		$^{207}\text{Pb}/^{235}\text{U}$		$^{206}\text{Pb}/^{238}\text{U}$									
	(ppm)	(ppm)																								
		Isotopic ratios																								
HSW6-12-01	408	706	0.58	0.052	0.95	0.001	4	0.339	0.32	0.008	8	0.046	22	0.000	4	327	44	297	7	291	2					
HSW6-12-02	312	682	0.46	0.062	0.08	0.001	5	0.397	0.80	0.009	4	0.046	18	0.000	4	677	36	340	7	291	2					
HSW6-12-03	204	4291	0.05	0.049	0.15	0.000	9	0.198	0.29	0.003	6	0.029	0.07	0.000	2	155	28	184	3	185	1					
HSW6-12-04	121	573	0.21	0.050	0.80	0.001	4	0.310	0.02	0.008	3	0.043	0.99	0.000	4	232	47	274	6	278	2					
HSW6-12-05	356	626	0.57	0.055	0.78	0.001	9	0.307	0.73	0.010	5	0.039	0.73	0.000	4	444	57	272	8	251	3					
HSW6-12-06	123	238	0.52	0.061	0.62	0.002	5	0.392	0.66	0.015	6	0.046	16	0.000	5	661	66	336	11	291	3					
HSW6-12-07	192	400	0.48	0.050	0.08	0.005	3	0.197	0.43	0.020	0	0.028	0.59	0.000	8	199	236	183	17	182	5					
HSW6-12-08	1133	1751	0.65	0.054	0.09	0.001	0	0.381	0.23	0.007	7	0.050	0.82	0.000	4	375	32	328	6	320	2					
HSW6-12-09	169	257	0.66	0.061	0.16	0.003	0	0.389	0.08	0.018	4	0.046	27	0.000	4	645	85	334	13	292	3					
HSW6-12-10	253	321	0.79	0.055	0.15	0.006	0	0.330	0.98	0.035	5	0.043	0.52	0.000	9	418	250	290	27	275	6					
HSW6-12-11	393	594	0.66	0.058	0.75	0.001	9	0.409	0.19	0.011	6	0.050	0.76	0.000	6	558	43	348	8	319	3					
HSW6-12-12	585	736	0.79	0.053	0.09	0.002	1	0.341	0.70	0.013	1	0.046	54	0.000	6	333	65	298	10	293	3					
HSW6-12-13	670	843	0.80	0.053	0.56	0.001	4	0.341	0.51	0.008	6	0.046	21	0.000	3	353	44	298	7	291	2					
HSW6-12-14	144	268	0.54	0.053	0.74	0.002	5	0.342	0.11	0.015	5	0.046	32	0.000	5	360	83	299	12	292	3					
HSW6-12-15	680	1476	0.46	0.058	0.18	0.002	1	0.372	0.78	0.012	7	0.046	43	0.000	5	537	56	322	9	293	3					
HSW6-12-16	418	1523	0.27	0.059	0.58	0.001	6	0.327	0.23	0.009	2	0.039	0.75	0.000	4	589	45	287	7	251	2					
HSW6-12-17	239	623	0.38	0.054	0.02	0.002	1	0.294	0.81	0.010	8	0.039	0.74	0.000	5	372	62	262	8	251	3					
HSW6-12-18	122	287	0.42	0.058	0.47	0.002	8	0.369	0.79	0.018	1	0.046	18	0.000	7	547	79	319	13	291	4					
HSW6-12-19	604	696	0.87	0.052	0.84	0.001	9	0.337	0.68	0.012	5	0.046	18	0.000	4	322	69	295	9	291	2					
HSW6-12-20	270	557	0.48	0.053	0.72	0.001	5	0.342	0.71	0.009	9	0.046	24	0.000	5	359	45	299	7	291	3					
HSW6-12-21	616	1081	0.57	0.053	0.34	0.001	5	0.341	0.65	0.009	7	0.046	29	0.000	4	343	47	298	7	292	3					
HSW6-12-22	872	1382	0.63	0.052	0.19	0.002	2	0.331	0.30	0.013	3	0.046	0.04	0.000	4	294	96	291	10	290	3					
HSW6-12-23	309	525	0.59	0.058	0.46	0.001	9	0.367	0.25	0.010	4	0.046	21	0.000	6	547	40	318	8	291	3					
11HSW4-2-01	150	258	0.58	0.056	0.55	0.002	7	0.448	0.10	0.021	5	0.057	0.33	0.000	7	474	84	376	15	359	4					
11HSW4-2-02	59	131	0.45	0.076	0.20	0.005	2	0.402	0.80	0.024	9	0.040	67	0.000	9	529	257	281	27	253	6					
11HSW4-2-03	232	269	0.86	0.056	0.52	0.002	7	0.593	0.79	0.027	5	0.075	0.94	0.001	2	473	74	473	18	472	7					

Continued

Spot	^{232}Th (ppm)	^{238}U (ppm)	Th/U	Isotopic ratios						$^{206}\text{Pb}/^{235}\text{U}$						$^{206}\text{Pb}/^{238}\text{U}$					
				$^{207}\text{Pb}/^{206}\text{Pb}$			$^{207}\text{Pb}/^{235}\text{U}$			$^{206}\text{Pb}/^{238}\text{U}$			$^{207}\text{Pb}/^{206}\text{Pb}$			$^{207}\text{Pb}/^{235}\text{U}$			$^{206}\text{Pb}/^{238}\text{U}$		
				Ratio	1σ	Ratio	1σ	Ratio	1σ	Ratio	1σ	Age (Ma)	1σ	Age (Ma)	1σ	Age (Ma)	1σ	Age (Ma)	1σ		
11HSW4-2-04	392	636	0.62	0.054 31	0.002 4	0.303 70	0.012 7	0.040 63	0.000 6	384	69	269	10	257	4						
11HSW4-2-05	232	244	0.95	0.057 31	0.003 3	0.586 30	0.033 5	0.074 85	0.001 3	503	95	469	21	465	8						
11HSW4-2-06	85	138	0.62	0.056 15	0.003 9	0.560 28	0.036 7	0.072 81	0.001 5	458	110	452	24	453	9						
11HSW4-2-07	569	1 023	0.56	0.051 21	0.002 0	0.365 32	0.013 6	0.051 66	0.000 6	250	64	316	10	325	4						
11HSW4-2-08	430	531	0.81	0.051 80	0.002 4	0.291 55	0.014 1	0.040 54	0.000 6	277	83	260	11	256	4						
11HSW4-2-09	302	682	0.44	0.056 52	0.001 7	0.589 73	0.016 9	0.075 52	0.000 9	473	42	471	11	469	5						
11HSW4-2-10	345	620	0.56	0.051 28	0.002 6	0.287 94	0.013 8	0.040 64	0.000 6	254	82	257	11	257	4						
11HSW4-2-11	276	254	1.08	0.054 64	0.003 4	0.302 57	0.017 9	0.040 54	0.000 8	398	96	268	14	256	5						
11HSW4-2-12	320	313	1.02	0.055 73	0.003 1	0.500 12	0.026 3	0.066 28	0.001 2	441	84	412	18	414	7						
11HSW4-2-13	178	240	0.74	0.058 03	0.003 2	0.675 48	0.037 3	0.084 42	0.001 5	531	90	524	23	522	9						
11HSW4-2-14	312	503	0.62	0.055 98	0.002 0	0.588 91	0.021 6	0.075 35	0.001 0	452	58	470	14	468	6						
11HSW4-2-15	114	1 077	0.11	0.051 07	0.002 0	0.286 04	0.010 9	0.040 48	0.000 6	244	60	255	9	256	4						
11HSW4-2-16	148	232	0.64	0.054 66	0.004 0	0.298 34	0.021 3	0.040 43	0.000 8	398	123	265	17	255	5						
11HSW4-2-17	191	331	0.58	0.047 03	0.002 6	0.305 73	0.016 7	0.046 73	0.000 7	51	91	271	13	294	4						
11HSW4-2-18	394	769	0.51	0.055 88	0.002 2	0.313 97	0.011 6	0.040 62	0.000 5	304	135	260	13	255	3						
11HSW4-2-19	579	789	0.73	0.051 32	0.001 9	0.286 88	0.010 3	0.040 44	0.000 5	255	59	256	8	256	3						
11HSW4-2-20	170	384	0.44	0.054 58	0.002 9	0.295 23	0.014 3	0.039 74	0.000 7	395	78	263	11	251	4						
11HSW4-2-21	137	333	0.41	0.055 87	0.002 6	0.394 67	0.018 9	0.050 77	0.000 8	447	79	338	14	319	5						
11HSW4-2-22	293	319	0.92	0.053 88	0.003 5	0.298 06	0.018 1	0.041 16	0.001 1	366	90	265	14	260	7						
11HSW4-2-23	214	409	0.52	0.054 31	0.002 6	0.300 18	0.013 3	0.040 30	0.000 6	384	74	267	10	255	4						
11HSW4-2-24	396	857	0.46	0.055 01	0.002 2	0.306 46	0.011 6	0.040 63	0.000 6	413	60	271	9	257	3						
11HSW4-2-25	170	296	0.57	0.053 03	0.004 4	0.357 57	0.026 3	0.050 25	0.001 1	330	129	310	20	316	7						
11HSW4-2-26	92	178	0.52	0.046 84	0.004 2	0.295 70	0.025 2	0.045 78	0.001 1	41	196	263	20	289	7						
11HSW4-2-27	261	409	0.64	0.052 16	0.003 4	0.290 12	0.018 2	0.040 57	0.000 7	292	110	259	14	256	4						
11HSW4-2-28	144	268	0.54	0.057 09	0.003 5	0.314 73	0.018 2	0.040 95	0.000 7	495	99	278	14	259	4						
11HSW4-2-29	149	314	0.47	0.052 32	0.004 9	0.357 42	0.033 3	0.049 55	0.000 8	299	216	310	25	312	5						

Continued

Spot	^{232}Th (ppm)	^{238}U (ppm)	Th/U	Isotopic ratios						$^{207}\text{Pb}/^{206}\text{Pb}$	$^{206}\text{Pb}/^{235}\text{U}$	$^{207}\text{Pb}/^{206}\text{Pb}$	$^{206}\text{Pb}/^{238}\text{U}$	$^{207}\text{Pb}/^{206}\text{Pb}$	$^{206}\text{Pb}/^{235}\text{U}$	$^{206}\text{Pb}/^{238}\text{U}$								
				$^{207}\text{Pb}/^{206}\text{Pb}$		$^{207}\text{Pb}/^{235}\text{U}$		$^{206}\text{Pb}/^{238}\text{U}$																
				Ratio	1σ	Ratio	1σ	Ratio	1σ															
11HSW4-2-30	111	170	0.65	0.065 67	0.004 4	0.367 18	0.024 4	0.040 56	0.000 9	796	103	318	18	256	5									
11HSW4-2-31	323	558	0.58	0.053 43	0.002 3	0.301 45	0.013 2	0.040 60	0.000 6	347	72	268	10	257	4									
11HSW4-2-32	174	375	0.46	0.055 58	0.003 1	0.359 56	0.020 9	0.046 35	0.000 9	436	95	312	16	292	6									
11HSW4-2-33	134	479	0.28	0.053 11	0.002 9	0.331 89	0.017 1	0.045 73	0.000 7	333	90	291	13	288	4									
11HSW4-2-34	234	364	0.64	0.063 63	0.002 9	0.767 95	0.031 8	0.088 03	0.001 3	729	62	579	18	544	8									
11HSW4-2-35	292	640	0.46	0.052 47	0.002 4	0.297 46	0.013 9	0.040 80	0.000 6	306	80	264	11	258	4									
11HSW4-2-36	131	263	0.50	0.056 16	0.003 4	0.355 57	0.021 7	0.046 38	0.000 9	459	101	309	16	292	6									
11HSW4-2-37	245	320	0.77	0.057 55	0.003 0	0.320 21	0.016 9	0.040 11	0.000 7	513	86	282	13	253	4									
11HSW4-2-38	313	731	0.43	0.051 67	0.002 3	0.293 94	0.012 9	0.040 83	0.000 6	271	75	262	10	258	4									
11HSW4-2-39	317	414	0.77	0.048 98	0.002 4	0.348 57	0.016 9	0.051 40	0.001 0	147	78	304	13	323	6									
11HSW4-2-40	281	315	0.89	0.055 19	0.002 9	0.691 55	0.035 4	0.089 81	0.001 3	420	88	534	21	554	8									
11HSW4-2-41	64	77	0.83	0.072 85	0.006 1	0.394 64	0.030 9	0.040 62	0.001 1	1 010	114	338	23	257	7									
11HSW4-2-42	131	261	0.50	0.056 52	0.004 5	0.307 31	0.022 6	0.039 93	0.000 9	473	125	272	18	252	5									
11HSW4-2-43	256	273	0.94	0.057 26	0.004 0	0.370 49	0.028 3	0.046 01	0.000 9	501	135	320	21	290	5									
11HSW4-2-44	294	500	0.59	0.056 13	0.003 0	0.356 43	0.018 8	0.046 05	0.000 6	457	94	310	14	290	4									
11HSW4-2-45	175	348	0.50	0.059 01	0.003 8	0.371 79	0.024 1	0.045 53	0.000 8	567	110	321	18	287	5									
11HSW4-2-46	257	300	0.86	0.055 98	0.005 4	0.477 86	0.039 7	0.063 02	0.001 1	452	154	397	27	394	7									
11HSW4-2-47	156	319	0.49	0.053 21	0.003 4	0.333 46	0.020 6	0.046 11	0.000 7	338	111	292	16	291	5									
11HSW4-2-48	227	424	0.54	0.055 50	0.002 5	0.499 10	0.020 4	0.065 87	0.000 9	432	66	411	14	411	6									
11HSW4-2-49	727	932	0.78	0.064 22	0.004 2	0.359 08	0.021 9	0.040 74	0.000 7	329	243	261	24	254	5									
11HSW4-2-50	589	1 065	0.55	0.053 79	0.002 8	0.377 29	0.020 4	0.050 40	0.000 8	362	95	325	15	317	5									
11HSW4-2-51	222	378	0.59	0.057 76	0.002 5	0.674 84	0.030 6	0.084 05	0.001 2	521	74	524	19	520	7									
11HSW4-2-52	73	194	0.37	0.060 26	0.003 3	0.688 07	0.037 1	0.083 56	0.001 3	613	90	532	22	517	8									

six age populations: 256 ± 2 ($n=23$, 1σ), 290 ± 3 ($n=9$, 1σ), 319 ± 4 ($n=6$, 1σ), 412 ± 9 ($n=2$, 1σ), 469 ± 6 ($n=4$, 1σ), and 520 ± 9 Ma ($n=3$, 1σ) (Fig. 5b, Table 1). The above two samples have similar age association, implying that they have similar provenance. Additionally, the youngest age (255 Ma) in them is interpreted to represent the maximum depositional age of the protoliths of these leptynites (Fig. 5f).

Gneissic Biotite Syenogranite

The zircons from the two gneissic biotite syenogranites (HSW6-4 and HSW6-12) are euhedral-subhedral in shape, and display oscillatory growth zoning in CL images (Figs. 4c and 4d), implying a magmatic origin. The $^{206}\text{Pb}/^{238}\text{U}$ ages of 25 analytical spots of sample HSW6-4 range from 177 to 336 Ma (Table

1), yielding weighted mean $^{206}\text{Pb}/^{238}\text{U}$ age of 183 ± 2 ($n=12$, 1σ), 225 ± 3 ($n=3$, 1σ), 249 ± 6 ($n=3$, 1σ), 291 ± 3 ($n=4$, 1σ), and 321 ± 7 ($n=1$) as well as 336 ± 7 Ma ($n=1$) (Fig. 5c). The $^{206}\text{Pb}/^{238}\text{U}$ ages of 23 analytical spots of sample HSW6-12 range from 182 to 320 Ma, yielding age populations of 185 ± 2 ($n=2$, 1σ), 251 ± 3 ($n=3$, 1σ), 278 ± 4 ($n=2$, 1σ), 291 ± 1 ($n=14$, 1σ), and 320 ± 3 Ma ($n=2$, 1σ) (Fig. 5d, Table 1). Their youngest ages (183 ± 2 and 185 ± 2 Ma) for these two samples are the same within uncertainty, considered to represent the crystallization age of the gneissic biotite syenogranite, i.e., Early Jurassic, rather than the previously believed Neoproterozoic (HBGMR, 1993). In addition, the other ages are interpreted as the crystallization ages of inherited or captured zircons entrained in the gneissic biotite syenogranite, consistent with the ages of the



Figure 4. CL images of the selected zircons from the Fengshuigouhe Group in the study area.

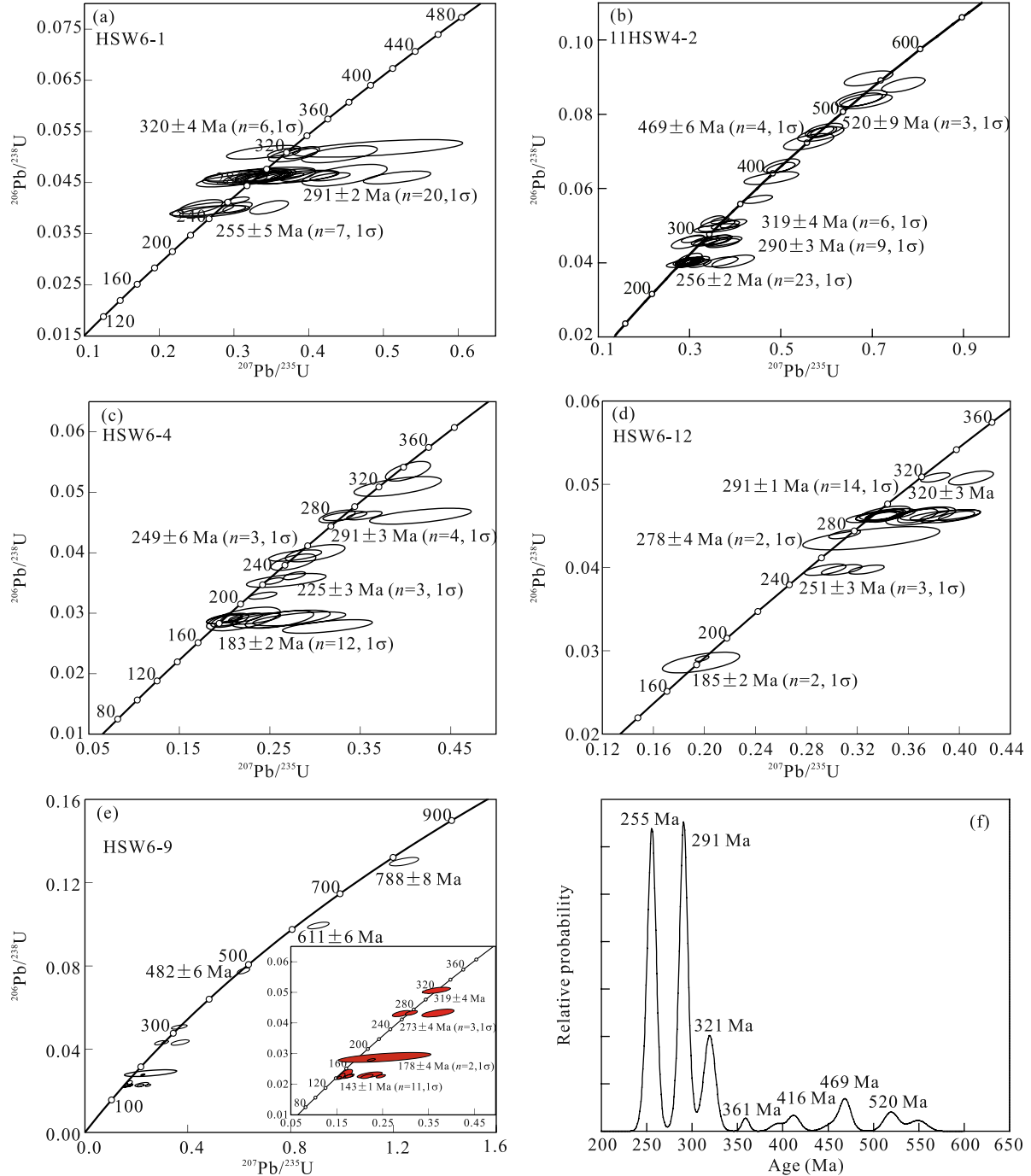


Figure 5. Zircon U-Pb concordia diagrams for the samples and relative probability plot of detrital zircons from the Fengshuigouhe Group.

detrital zircons from biotite leptynites.

Granitic Pegmatite

Two main types of zircons can be recognized for the granitic pegmatite (HSW6-9) based on their shape and inner structure in CL images. Type-1 zircons are subhedral in shape and display oscillatory zoning, suggesting a magmatic origin. Type-2 zircons display

structureless in CL images and have high Th, U contents (Fig. 4e, Table 1), implying their hydrothermal origin (Wu and Zheng, 2004). The dating results indicate that 11 analytical spots of hydrothermal zircons yield a weighted mean $^{206}\text{Pb}/^{238}\text{U}$ age of 143 ± 1 Ma, whereas the ages of other 9 spots rang from 178 to 788 Ma (Fig. 5e, Table 1). The former is interpreted to represent the formation age of the granitic pegmatite,

whereas the latter represents as the formation ages of captured zircons from the granitic pegmatite.

DISCUSSIONS

Rock Association and Age of the Fengshuigouhe Group

“The previous Fengshuigouhe Formation” was renamed as the Fengshuigouhe Group by HBGMR (1993), which is characterized by occurrence of staurolite, similar to the Majiajie and Luomahu groups assigned to the Neoproterozoic (HBGMR, 1993). The Fengshuigouhe Group, as one formation of the Xinkailing Group, was believed to form in Pre-Ordovician in 1 : 200 000 Regional Geological Survey (Fig. 1b) (Longzhen Commune Sheet, HBGMR, 1978), whereas in another sheet 1 : 200 000 Regional Geological Survey (Sunwu County Sheet), it was considered to form in the Paleoproterozoic (Fig. 1c) (HBGMR, 1991). Owing to the intensive covering of vegetation, and the lack of biochronological data, the formation age of the Fengshuigouhe Group remains controversial. However, the field relationship and new dating results provide strong constraints on the formation time of the group.

First, field observation indicates that the Fengshuigouhe Group, located near Xigangzi Town of Sunwu County and the standard section in the northeastern of Maihai Commune (HBGMR, 1993), is composed mainly of leptynite and gneissic granite. The former displays typical layer structure, implying their sedimentary origin. The latter exhibits gneissic structure and intruded into leptynite, suggesting that they are late intrusion, rather than previously believed gneiss (HBGMR, 1993, 1991, 1987). Meanwhile, this intrusive relationship shows that the Fengshuigouhe Group formed before the intrusion of the granite.

Second, zircons from the two leptynites (HSW6-1 and 11HSW4-2) give several age populations, the youngest age populations such as 255 ± 5 and 256 ± 2 Ma can be considered to be the maximum depositional ages of the Fengshuigouhe Group. Zircons from the gneissic biotite syenogranites intruding leptynites give 183–185 Ma ages, i.e., the Early Jurassic, consistent with widespread occurrence of Early Jurassic granitoids in NE China (Tang et al., 2011; Wu et al., 2011, 2002; Pei et al., 2008; Sui et al., 2007).

Meanwhile, this age (~ 185 Ma) can be considered to represent the sedimentary upper limit of the Fengshuigouhe Group.

Taking all the above information into account, we conclude that the protoliths of leptynites from the Fengshuigouhe Group formed between Late Permian (~ 255 Ma) to Early Jurassic (~ 185 Ma), rather than Neoproterozoic, as previously reported (HBGMR, 1993, 1991, 1978).

Provenance of the Fengshuigouhe Group

The detrital zircons from the Fengshuigouhe Group give an age ranging from 249 to 544 Ma, with peaks at 255, 290, 320, 469 and 520 Ma (Fig. 5f). Combined with their CL images (Figs. 4a and 4b) and Th/U ratios (Table 1), we consider that the ages from the detrital zircons should represent the time of early magmatic events.

The age peak at ~ 255 Ma is consistent with the zircon U-Pb dating results for the Songmushan alkaline granitoid and the Guguhe syenogranite in the Xing'an massif in the northwestern Lesser Xing'an Range (Wu et al., 2011, 2002; Sun et al., 2000). The ~ 290 Ma age population matches with the age of the Daheishan alkaline granitoids in the northern Great Xing'an Range (Wu et al., 2011, 2002; Sun et al., 2000). The Middle–Late Carboniferous magmatisms (~ 320 Ma) widely occur in NE China, especially near the northwestern Lesser Xing'an Range (Wu et al., 2011; Zhang et al., 2010; Zhao et al., 2010; Gao et al., 2007). The Middle Ordovician (~ 469 Ma) magmatic events such as the Baiyinna biotite granodiorite, Chalabanhe monzogranite and Halabaqi granite are also widely reported in this area and adjacent regions (Ge et al., 2007; Sui et al., 2006). The ~ 520 Ma magmatic events exist in each microcontinental massif in NE China (Zhou et al., 2012, 2010; Wu et al., 2011, 2005; Wilde et al., 2003, 2000).

Taken together, it is suggested that these ages of the detrital zircons from the Fengshuigouhe Group are consistent with the ages of igneous rocks in this study area and adjacent regions. The CL images of the detrital zircons indicate that they have low round degree, implying their short distance convey, i.e., the sediments in the Fengshuigouhe Group were sourced directly from geological bodies located on the surface in

the study area and adjacent regions and quickly accumulated.

CONCLUSIONS

The following conclusions are based on the geochronology of selected rocks from the Fengshuigouhe Group in the northwestern Lesser Xing'an Range.

(1) The Fengshuigouhe Group is composed mainly of a suit of metamorphic rocks (such as biotite leptynite) and gneissic granite intruding into leptynite.

(2) The protoliths of leptynites from the Fengshuigouhe Group formed between Late Paleozoic and Early Jurassic, rather than Neoproterozoic, as previously believed.

(3) The sediments of the biotite leptynites from the Fengshuigouhe Group were sourced directly from the geological bodies located on the surface in the study area and adjacent regions.

ACKNOWLEDGMENTS

We appreciate the assistance of the Langfang Geological Survey of Hebei Province for technical support in selecting the zircons. We thank the staff of the State Key Laboratory of Geological and Mineral Resources, China University of Geosciences, Wuhan, China, for their advice and assistance during U-Pb zircon dating using LA-ICP-MS. This study was financially supported by the National Natural Science Foundation of China (No. 41072038), China Geological Survey (No. 1212010070301), and the Opening Foundation of the State Key Laboratory of Geological Processes and Mineral Resources, China University of Geosciences, Wuhan.

REFERENCES CITED

- Anderson, T., 2002. Correction of Common Lead in U-Pb Analyses that do not Report ^{204}Pb . *Chemical Geology*, 192: 59–79, doi:10.1016/S0009-2541(02)00195-X
- Chen, B., Jahn, B. M., Tian, W., 2009. Evolution of the Songliao Suture Zone: Constraints from Zircon U-Pb Ages, Hf Isotopic Ratios and Whole-Rock Nd-Sr Isotope Compositions of Subduction- and Collision-Related Magmas and Forearc Sediments. *Journal of Asian Earth Sciences*, 34(3): 245–257, doi:10.1016/j.jseas.2008.05.007
- Gao, F. H., Xu, W. L., Yang, D. B., et al., 2007. LA-ICP-MS Zircon U-Pb Dating from Granitoids in Southern Basement of Songliao Basin: Constraints on Ages of the Basin Basement. *Science in China (Series D)*, 50(7): 995–1004, doi:10.1007/s11430-007-0019-7
- Ge, W. C., Sui, Z. M., Wu, F. Y., et al., 2007. Zircon U-Pb Ages, Hf Isotopic Characteristics and Their Implications of the Early Paleozoic Granites in the Northeastern Da Hinggan Mts., Northeastern China. *Acta Petrologica Sinica*, 23(2): 423–440, doi:10.1000-0569/2007/023(02)-0423-4 (in Chinese with English Abstract)
- HBGMR (Heilongjiang Bureau of Geology and Mineral Resources), 1978. Report of 1 : 200 000 Regional Geological Research (Longzhen Commune Sheets) (in Chinese)
- HBGMR, 1991. Report of 1 : 200 000 Regional Geological Research (Sunwu County Sheets). Geological Publishing House, Beijing. (in Chinese)
- HBGMR, 1993. Regional Geology of Heilongjiang Province. Geological Publishing House, Beijing. 1–734 (in Chinese with English Abstract)
- IMBGMR (Inner Mongolia Bureau of Geology and Mineral Resources), 1991. Regional Geology of Inner Mongolia. Geological Publishing House, Beijing. 1–725 (in Chinese with English Abstract)
- Li, J. Y., Niu, B. G., Song, B., et al., 1999. Crustal Formation and Evolution of Northern Changbai Mountains, Northeast China. Geological Publishing House, Beijing. 1–136 (in Chinese with English Abstract)
- Li, J. Y., 2006. Permian Geodynamic Setting of Northeast China and Adjacent Regions: Closure of the Paleo-Asian Ocean and Subduction of the Paleo-Pacific Plate. *Journal of Asian Earth Sciences*, 26(3–4): 207–224, doi:10.1016/j.jseas.2005.09.001
- Liu, Y. S., Hu, Z. C., Gao, S., et al., 2008. In Situ Analysis of Major and Trace Elements of Anhydrous Minerals by LA-ICP-MS without Applying an Internal Standard. *Chemical Geology*, 257(1–2): 34–43, doi:10.1016/j.chemgeo.2008.08.004
- Liu, Y. S., Gao, S., Hu, Z. C., et al., 2010a. Continental and Oceanic Crust Recycling-Induced Melt-Peridotite Interactions in the Trans-North China Orogen: U-Pb Dating, Hf Isotopes and Trace Elements in Zircons from Mantle Xenoliths. *Journal of Petrology*, 51(1–2): 537–571, doi:10.1093/petrology/egp082
- Liu, Y. S., Hu, Z. C., Zong, K. Q., et al., 2010b. Reappraisal and Refinement of Zircon U-Pb Isotope and Trace Element Analyses by LA-ICP-MS. *Chinese Science Bulletin*

- tin*, 55(15): 1535–1546, doi:10.1007/s11434-010-3052-4
- Ludwig, K. R., 2003. ISOPLOT 3.00: A Geochronological Toolkit for Microsoft Excel. *Berkeley Geochronology Center Special Publication*, 4: 74
- Miao, L. C., Fan, W. M., Zhang, F. Q., et al., 2003. SHRIMP Zircon Geochronology and Its Implications on the Xinkailing-Keluo Complex, Northwestern of Lesser Xing'an Range. *Chinese Science Bulletin*, 48(22): 2315–2323 (in Chinese)
- Miao, L. C., Liu, D. Y., Zhang, F. Q., et al., 2007. Zircon SHRIMP U-Pb Ages of the “Xinghuadukou Group” in Hanjiayuanzi and Xinlin Areas and the “Zhalantun Group” in Inner Mongolia, Da Hinggan Mountains. *Chinese Science Bulletin*, 52(8): 1112–1124, doi:10.1007/s11434-007-0131-2
- Pei, F. P., Xu, W. L., Meng, E., et al., 2008. The Beginning of the Paleo-Pacific Plate Subduction: Geochronological and Geochemical Evidence from the Early–Middle Jurassic Volcanic Rocks in the Eastern of Jilin and Heilongjiang Provinces. *Bulletin of Mineralogy, Petrology and Geochemistry*, 27(Suppl. I): 268 (in Chinese)
- Shi, G. H., Miao, L. C., Zhang, F. Q., et al., 2004. The Age and Its District Tectonic Implications on the Xilinhaote A-Type Granites, Inner Mongolia. *Chinese Science Bulletin*, 49(4): 384–389 (in Chinese)
- Sui, Z. M., Ge, W. C., Wu, F. Y., et al., 2006. U-Pb Chronology in Zircon from Harahaqi Granitic Pluton in Northeastern Daxing'anling Area and Its Origin. *Global Geology*, 25(3): 229–236 (in Chinese with English Abstract)
- Sui, Z. M., Ge, W. C., Wu, F. Y., et al., 2007. Zircon U-Pb Ages, Geochemistry and Its Petrogenesis of Jurassic Granites in Northeastern Part of the Da Hinggan Mts.. *Acta Petrologica Sinica*, 23(2): 461–480 (in Chinese with English Abstract)
- Sun, D. Y., Wu, F. Y., Li, H. M., et al., 2000. Emplacement Age of the Postorogenic A-Type Granites in Northwestern Lesser Xing'an Ranges, and Its Relationship to the Eastward Extension of Suolushan-Hegenshan-Zhalaite Collisional Suture Zone. *Chinese Science Bulletin*, 46(5): 427–432, doi:10.1007/BF03183282
- Tang, J., Xu, W. L., Wang, F., et al., 2011. Petrogenesis of Bimodal Volcanic Rocks from Maoershan Formation in Zhangguangcai Range: Evidence from Geochronology and Geochemistry. *Global Geology*, 30(4): 508–520, doi:10.3969/j.issn.1004-5589.2011.04.002 (in Chinese with English Abstract)
- Wang, F., Xu, W. L., Meng, E., et al., 2011. Early Paleozoic Amalgamation of the Songnen-Zhangguangcai Range and Jiamusi Massifs in the Eastern Segment of the Central Asian Orogenic Belt: Geochronological and Geochemical Evidence from Granitoids and Rhyolites. *Journal of Asian Earth Science*, 49: 234–248, doi:10.1016/j.jseas.2011.09.022
- Wang, F., Xu, W. L., Gao, F. H., et al., 2012. Tectonic History of the Zhangguangcailing Group in Eastern Heilongjiang Province, NE China: Constraints from U-Pb Geochronology of Detrital and Magmatic Zircons. *Tectonophysics*, 566–567: 105–122, doi:10.1016/j.tecto.2012.07.018
- Wilde, S. A., Zhang, X. Z., Wu, F. Y., 2000. Extension of a Newly Identified 500 Ma Metamorphic Terrane in North East China: Further U-Pb SHRIMP Dating of the Mashan Complex, Heilongjiang Province, China. *Tectonophysics*, 328: 115–130, doi:10.1016/S0040-1951(00)00180-3
- Wilde, S. A., Wu, F. Y., Zhang, X. Z., 2003. Late Pan-African Magmatism in Northeastern China: SHRIMP U-Pb Zircon Evidence from Granitoids in the Jiamusi Massif. *Precambrian Research*, 122: 311–327, doi:10.1016/S0301-9268(02)00217-6
- Wu, F. Y., Sun, D. Y., Li, H. M., et al., 2002. A-Type Granites in Northeastern China: Age and Geochemical Constraints on Their Petrogenesis. *Chemical Geology*, 187: 143–173, doi:10.1016/S0009-2541(02)00018-9
- Wu, F. Y., Yang, J. H., Lo, C. H., et al., 2007a. The Heilongjiang Group: A Jurassic Accretionary Complex in the Jiamusi Massif at the Western Pacific Margin of Northeastern China. *Island Arc*, 16: 156–172, doi:10.1111/j.1440-1738.2007.00564.x
- Wu, F. Y., Zhao, G. C., Sun, D. Y., et al., 2007b. The Hulan Group: Its Role in the Evolution of the Central Asian Orogenic Belt of NE China. *Journal of Asian Earth Sciences*, 30: 542–556, doi:10.1016/j.jseas.2007.01.003
- Wu, F. Y., Sun, D. Y., Ge, W. C., et al., 2011. Geochronology of the Phanerozoic Granitoids in Northeastern China. *Journal of Asian Earth Sciences*, 41: 1–30, doi:10.1016/j.jseas.2010.11.014
- Wu, G., Sun, F. Y., Zhao, C. S., et al., 2005. Discovery of the Early Paleozoic Post-Collisional Granites in Northern Margin of the Erguna Massif and Its Geological Significance. *Chinese Science Bulletin*, 50(23): 2733–2743, doi:10.1007/BF02899644
- Wu, Y. B., Zheng, Y. F., 2004. Genesis of Zircon and Its Constraints on Interpretation of U-Pb Age. *Chinese Science*

- Bulletin, 49(15): 1554–1569, doi:10.1007/BF03184122
- Xu, W. L., Ji, W. Q., Pei, F. P., et al., 2009. Triassic Volcanism in Eastern Heilongjiang and Jilin Provinces, NE China: Chronology, Geochemistry, and Tectonic Implications. *Journal of Asian Earth Sciences*, 34: 392–402, doi:10.1016/j.jseaes.2008.07.001
- Zhang, Y. L., Ge, W. C., Gao, Y., et al., 2010. Zircon U-Pb Ages and Hf Isotopes of Granites in Longzhen Area and Their Geological Implications. *Acta Petrologica Sinica*, 26(4): 1059–1073 (in Chinese with English Abstract)
- Zhao, Z., Chi, X. G., Pan, S. Y., et al., 2010. Zircon U-Pb LA-ICP-MS Dating of Carboniferous Volcanics and Its Geological Significance in the Northwestern Lesser Xing’an Range. *Acta Petrologica Sinica*, 26(8): 2452–2464 (in Chinese with English Abstract)
- Zhou, J. B., Wilde, S. A., Zhang, X. Z., et al., 2009. The Onset of Pacific Margin Accretion in NE China: Evidence from the Heilongjiang High-Pressure Metamorphic Belt. *Tectonophysics*, 478: 230–246, doi:10.1016/j.tecto.2009.08.009
- Zhou, J. B., Wilde, S. A., Zhao, G. C., et al., 2010. Was the Easternmost Segment of the Central Asian Orogenic Belt Derived from Gondwana or Siberia: An Intriguing Dilemma? *Journal of Geodynamics*, 50: 300–317, doi:10.1016/j.jog.2010.02.004
- Zhou, J. B., Wilde, S. A., Zhang, X. Z., et al., 2012. Detrital Zircons from Phanerozoic Rocks of the Songliao Block, NE China: Evidence and Tectonic Implications. *Journal of Asian Earth Sciences*, 47: 21–34, doi:10.1016/j.jseaes.2011.05.004